Available online at www.sciencedirect.com
ScienceDirect
Earth and Planetary Science Letters 268 (2008) 339–353
EPSL
www.elsevier.com/locate/epsl

Exchange bias identifies lamellar magnetism as the origin of the natural remanent magnetization in titanohematite with ilmenite exsolution from Modum, Norway

Karl Fabian [a,*], Suzanne A. McEnroe [a], Peter Robinson [a], Valera P. Shcherbakov [b]

[a] *Geological Survey of Norway, Leiv Eirikssons vei 39, N-7491 Trondheim, Norway*
[b] *Geophysical Observatory 'Borok', Yaroslavskaja Oblast, 151742, Russia*

Received 13 June 2007; received in revised form 13 December 2007; accepted 20 January 2008
Available online 12 February 2008
Editor: G.D. Price

Abstract

Large and stable negative magnetic anomalies in southwestern Sweden, southern Norway, the Adirondacks, USA, and Quebec, Canada, are related to rock units with a magnetic fraction consisting primarily of ilmeno-hematite or hemo-ilmenite. It has been suggested that the unusual magnetic stability of these rocks results from lamellar magnetism. This is a type of magnetic remanence, carried by uncompensated magnetic layers at interfaces between nanoscale exsolution structures of antiferromagnetic (AFM) hematite and paramagnetic ilmenite. Here we present the first direct proof that this lamellar magnetism indeed is responsible for the natural remanent magnetization (NRM) of a rock from Modum, Norway. Our argument expands a previous observation, that, in mineral grains from this rock, the cooling of a positive-induced remanence from room temperature to 5 K – which is well below the ordering temperature of ilmenite (57 K) – leads to a large negative shift of the low-temperature (LT) hysteresis loop. This can only be explained by exchange bias due to exchange coupling across the hematite–ilmenite interfaces. In a different experiment, we now have cooled the original NRM of untreated grains to 5 K, and then measured the hysteresis loop. Again, in several separate grains we observed large shifts of the hysteresis curves. This shows that exchange bias develops also from the untreated NRM. This observation proves that the moments, which carry the NRM, also participate in the exchange coupling at the hematite–ilmenite interfaces. Therefore, the NRM is not carried by defect moments or stress-induced moments, which occur in normal bulk hematite. A closer look at the NRM-induced LT loops shows that exchange bias acts in both field directions, though one direction is clearly predominant. This observation can be interpreted as a frozen equilibrium of different proportions of oppositely directed lamellar moments, a key feature of the original lamellar magnetism hypothesis. We discuss lamellar aggregation, and the formation of exchange-coupled clusters to explain the observed high efficiency of lamellar NRM. We also conclude that remanence carried by lamellar moments should not be used for paleointensity estimates of terrestrial or extraterrestrial material.

Keywords: hematite; ilmenite; lamellar magnetism; exsolution

1. Introduction and background

1.1. Large negative crustal anomalies

Large magnetic anomalies are generally positive on an absolute scale, e.g. parallel to the Earth's internally generated field, because the presence of magnetic minerals in the crust usually leads to a field amplification by induced magnetization. Negative anomalies on an absolute scale can occur only if the natural remanence of the rocks is inverse to the field and overcomes the induced moment.

Rock units wherein the magnetic fraction consists primarily of ilmeno-hematite have been found at large and stable negative magnetic anomalies in granulite-facies rocks in the Adirondacks, New York (Balsley and Buddington, 1958; McEnroe and Brown, 2000), and in upper amphibolite-facies rocks in southern Sweden and Norway (McEnroe et al., 2001, 2007a). Remanent anomalies

* Corresponding author.
E-mail address: karl.fabian@ngu.no (K. Fabian).

0012-821X/$ - see front matter © 2008 Elsevier B.V. All rights reserved.
doi:10.1016/j.epsl.2008.01.034

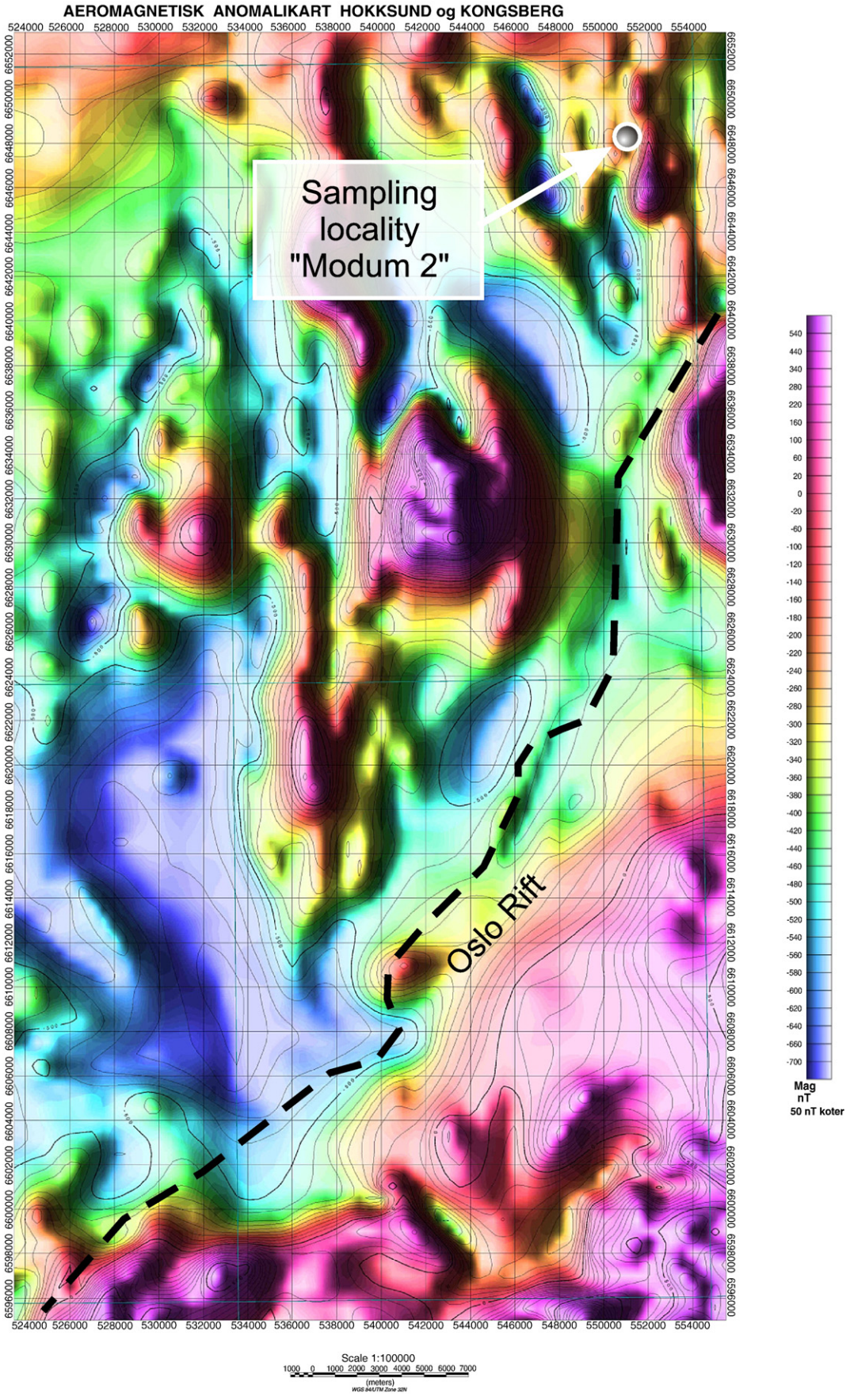

Fig. 1. Aeromagnetic map of the Hokksund and Kongsberg area, Norway. All our measurements have been performed on mineral samples from sillimanite gneiss rocks in the area of the negative magnetic anomaly over the Modum district.

also occur over areas with less oxidized igneous rocks in Norway and in Canada containing hemo-ilmenite +/− magnetite (McEnroe et al., 2002; Hargraves, 1959; Carmichael, 1959, 1961), and in granulite rocks in Sweden which contain both hemo-ilmenite and ilmeno-hematite +/− magnetite (McEnroe et al., 2001).

These exsolved rhombohedral oxides have astonishing magnetic properties which have been related either to unbalanced magnetic moments at nanoscale exsolution interfaces observed in these mineral phases (McEnroe et al., 2002; Robinson et al., 2002, 2004; McEnroe et al., 2004a; Kasama et al., 2004), or to a chemical locking of a high-temperature mono-mineralic single-domain remanence (Kletetschka et al., 2002).

The importance of this type of magnetization arises first from the high thermal stability of the related natural remanence, which may contribute significantly to the total magnetization of the lower crust in the Earth, especially near and below the Curie depth of magnetite (McEnroe et al., 2004b). Second, the strong and stable remanence of ilmeno-hematite- or hemo-ilmenite-bearing units has been suggested as an explanation for the observed large Martian magnetic anomalies that persist even though Mars has no internally created field. Third, magnetic properties of ilmenite–hematite minerals have been studied for a long time in different contexts (Carmichael, 1961; Merrill, 1968; Hoffman, 1992), and understanding the physical origin of this remanence will help to judge its reliability as a carrier of paleofield information. Fourth, the physical mechanism of this extremely stable remanence could be of interest for designing highly stable magnetic storage devices.

Here we study the natural remanent magnetization of mineral samples that have been collected in the area of a negative magnetic anomaly over the 1 Gyr-old metamorphic complex in the Modum district, South Norway. Modum lies within Mesoproterozoic basement, west of the Permian Oslo Rift. The North–South anomalies in the aeromagnetic map of Fig. 1 are features of the basement. The southeastern part of the map is within the Rift.

Samples were collected in the context of a larger project on crustal magnetism in the Modum area. 253 samples were measured for NRM and susceptibility to evaluate the contributions of remanence and induced magnetization to the aeromagnetic signal (Fig. 1). Susceptibility values are low, on average ($7 \cdot 10^{-3}$ SI) and NRM values are relatively high for metamorphic rocks at 1.8 A/m. In the larger Modum study, the average Koenigsberger ratio (Q-ratio) is 92, with nearly 70% of the samples having Q-ratios above 10. Clearly, remanence dominates the crustal magnetic signature from this region.

1.2. Ilmeno-hematite and the hypothesis of lamellar magnetism

The ilmeno-hematite-bearing samples, the subject of this paper, make up a unit in the Modum area. These rocks carry a stable natural remanent magnetization (NRM) of ≈1 A/m with an upward pointing magnetic vector at a steep angle to the present field direction, while having a very low susceptibility ($1.6 \cdot 10^{-4}$ SI). This very low susceptibility indicates an extremely low concentration of magnetic oxides. Their remanence is considerably higher than the induced magnetization, resulting in high Q-ratios with an average of 165. The rocks investigated here are sillimanite–feldspar gneisses which contain minor amounts of ilmeno-hematite, an exsolved rhombohedral oxide with titanohematite (Ti-bearing Fe_2O_3) as a host, and trace amounts of Fe-bearing rutile (TiO_2) as shown in Fig. 2. The titanohematite host contains about 6–10% $FeTiO_3$ in solid solution and exsolved submicroscopic (~ 1 nm thick) exsolution lamellae of ilmenite ($FeTiO_3$), identified by a combination of magnetic measurements, transmission electron microscopy (TEM) and Mossbauer spectroscopy (McEnroe et al., 2007b).

Low-temperature demagnetization of the NRM of sample MODLB-2 (Fig. 3 (left)) indicates that hematite's Morin transition does not influence its NRM significantly, whereas the onset of ilmenite AFM ordering at $T_N \approx 57$ K is visible as a clear remanence drop in Fig. 3 (left). This implies that the ilmenite phase is magnetically coupled to the NRM carriers, and that this coupling is inverse. Interestingly, all coupling effects in

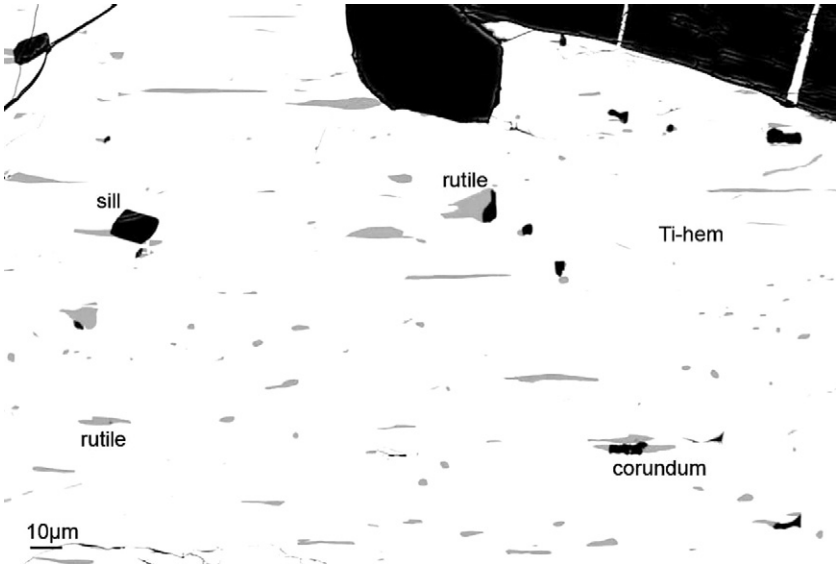

Fig. 2. SEM image of the seemingly homogenous titanohematite host with quartz contacts, sillimanite inclusions, and micrometer scale lamellae of rutile and corundum. The magnetic properties are dominated by nanometer scale ilmenite lamellae in the host, not observable at this scale.

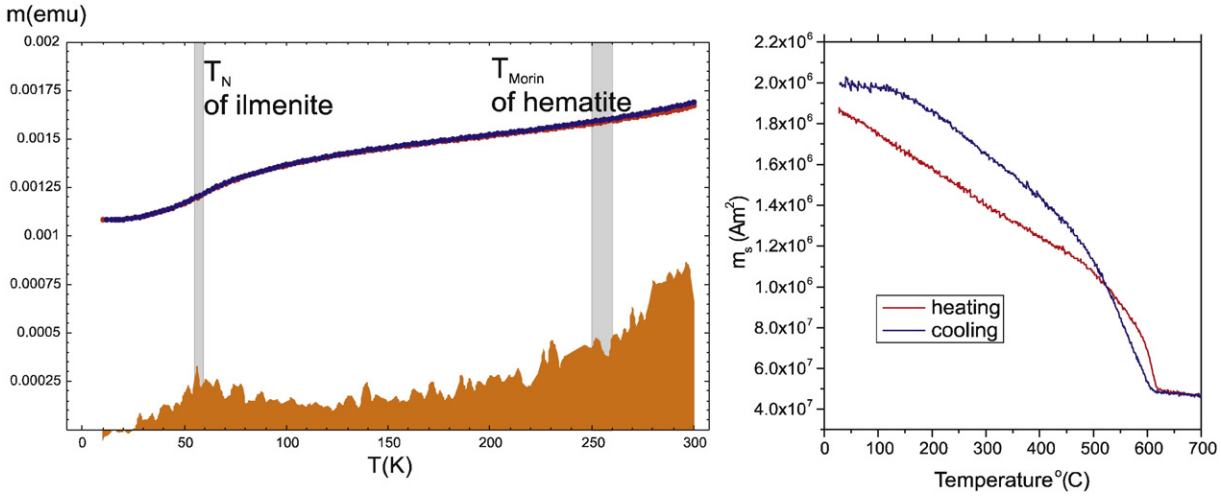

Fig. 3. A cooling–heating cycle for MODLB-02 (left) shows nearly 99% recovery of the NRM. The yellow area represents the amplified difference between cooling and heating curves (max = 1.3%). It shows a slight indication for loss at the Morin transition of hematite near 250 K, which is of little importance in absolute terms. In contrast, close to ilmenite's Néel temperature (T_N) the total magnetization drops clearly. Curie temperatures of Modum rocks (here MOD-2) lie between 610° and 620°C (right), common for $FeTiO_3$-substituted hematite. (For interpretation of the references to colour in this figure legend, the reader is referred to the web version of this article.)

Fig. 3 (left) are nearly completely reversible upon reheating the sample to RT. High-temperature measurements yield Curie temperatures between 610° and 620 °C (Fig. 3 (right)). During thermal demagnetization, the NRM of several rock samples unblocked between 610° and 615 °C.

Taken together, the above experiments show that the remanence is carried by titanohematite linked to ilmenite. Based further on the magnetic stability and high saturation magnetization of ilmeno-hematite bearing rocks, it has been suggested that their remanence results from uncompensated magnetic moments at interfaces between nanoscale exsolution lamellae of paramagnetic ilmenite in antiferromagnetic hematite (Robinson et al., 2002, 2004). This concept has been termed 'lamellar magnetism', and is supported by theoretical models which clearly show that ilmenite lamellae, embedded in a hematite host, lead to the proposed uncompensated (lamellar) moments in the antiferromagnetic hematite lattice.

While exsolution structures are abundant in the Modum rocks, it is inherently difficult to prove practically that the observed magnetization originates from lamellar magnetism. Other possibilities are 1) the canted antiferromagnetism (CAF) of $FeTiO_3$-substituted hematite, 2) classically assumed defect moments, attributed to stress centers or local uncompensated spins unrelated to ilmenite lamellae, or 3) a somehow fixed high-temperature mono-mineralic single-domain remanence as claimed by Kletetschka et al. (2002).

1.3. Exchange bias

A huge advance towards an experimental proof of lamellar magnetism was the discovery of large exchange bias in natural titanohematite from Modum, containing exsolution lamellae of ilmenite (McEnroe et al., 2007b). In this earlier study, an induced remanent magnetization (IRM) at room temperature, after cooling in zero-field through ilmenite's Néel temperature, was found to induce a large hysteresis shift in the direction opposite to the previously applied field. Such hysteresis shifts are intensively studied in thin film materials and so-called core-shell nanoparticles, where they are known to arise from exchange bias at an interface between a ferromagnetic (FM) and an antiferromagnetic (AFM) phase (Nogués and Schuller, 1999; Stamps, 2000; Nogués et al., 2005).

The large hysteresis shift of more than 1 T observed by McEnroe et al. (2007b) can also only be explained by exchange coupling across a phase boundary. It therefore proves that some magnetic phase boundaries are present and relevant for the total magnetic moment of the Modum samples, even though they are probably AFM–AFM, rather than FM–AFM interfaces.

Another unusual aspect of the exchange bias found by McEnroe et al. (2007b), and further elaborated in the next section, is that it is induced by a room-temperature remanence after zero-field cooling. Usually hysteresis shift is only found

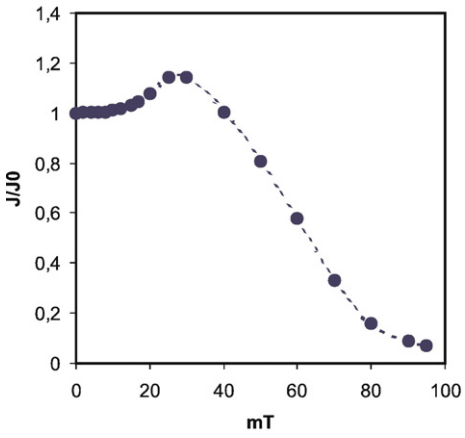

Fig. 4. Typical alternating-field (AF) demagnetization curve of a rock sample from Modum (Mod3-4a). Absolute remanence increases by about 20% between AF steps 15 and 30 mT, probably due to demagnetization of a relatively hard normal overprint over the reversed original NRM. The median destructive field is >60 mT and the sample is nearly demagnetized at 100 mT.

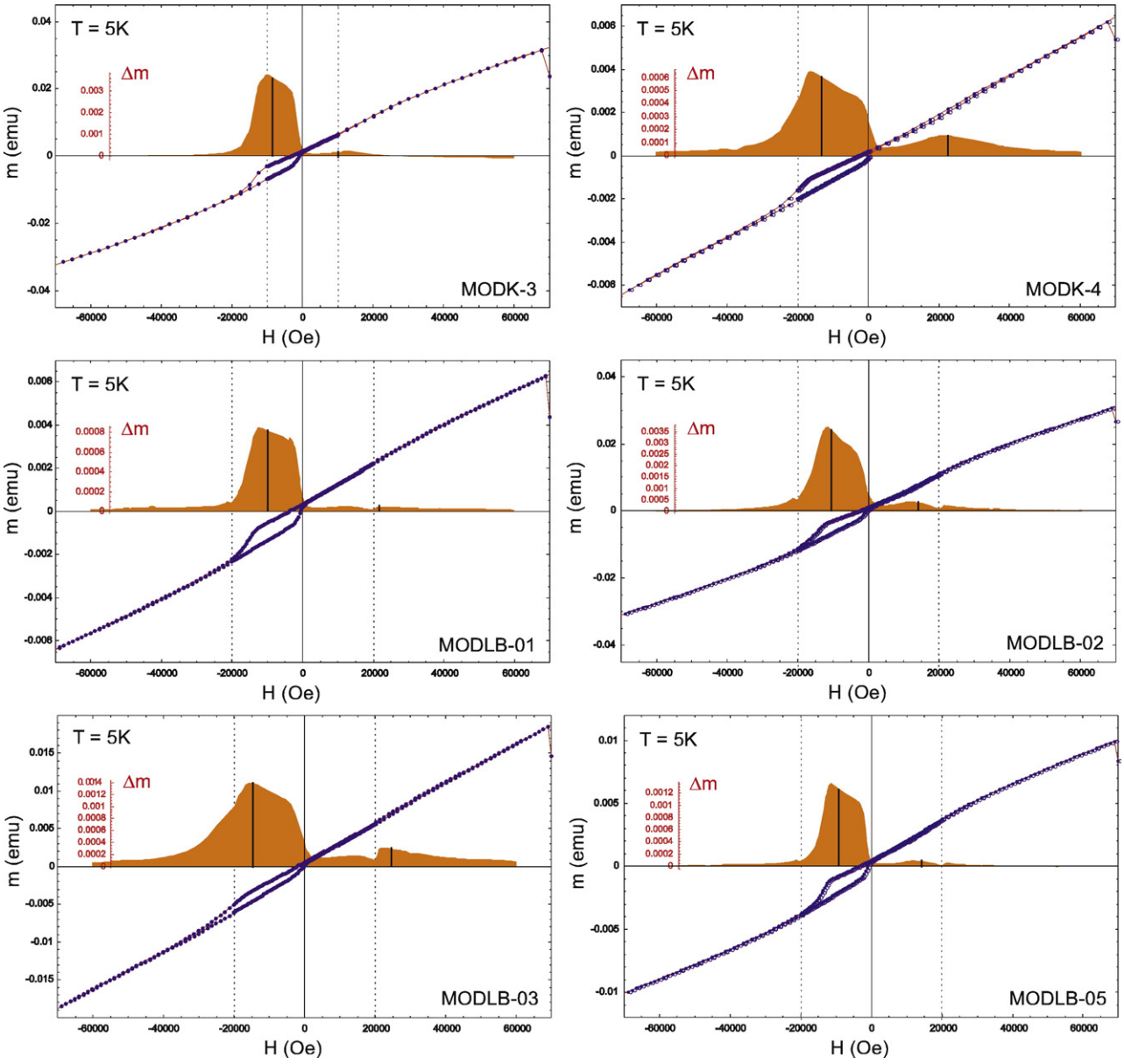

Fig. 5. Low-temperature hysteresis loops on six ilmeno-hematite mineral specimens from Modum. Samples were zero-field cooled after imposing a +7 T IRM at room temperature. The filled background plots display the amplified hysteresis differences which most clearly show the average bias field, here indicated by solid lines at the respective centers of mass. In all cases the average loop shift, H_E, is between 0.8 and 1.5 T. All loops have been measured to a maximum field of 7 T. Dashed vertical lines indicate the threshold field, where field step-size changed during the measurements. Sometimes a spurious step in the data occurs at these fields.

after cooling an FM–AFM couple in the presence of an external field through the AFM Néel temperature (Nogués et al., 2005). A typical system of FM Co-nanoparticle cores surrounded by oxidized AFM CoO shells shows no loop shift after zero-field cooling (Wen et al., 2004).

In the following, we will study the remanence-induced loop shift in detail, to verify experimentally the concept of lamellar magnetism as the carrier of the NRM in Modum samples.

2. Experimental methods and results

The experimental results in this section concern low-temperature measurements of hysteresis loops, which are obtained after cooling different magnetic RT remanences in zero-field. First, we reproduce the RT IRM results of McEnroe et al. (2007b) using different grains to show that they are typical for the selected rock samples from the Modum district. Second, we show measurements on zero-field cooled (ZFC) natural remanences, and interpret them in terms of bimodal loop shift. To support this explanation, we also produce a synthetic bimodal loop shift by ZFC of a partial IRM at RT.

2.1. Instruments

The high-temperature experiments reported here were performed either at the Institute of Rock Magnetism (IRM, Minnesota) or at the Norwegian Geological Survey (NGU, Trondheim) using a vibrating sample magnetometer equipped

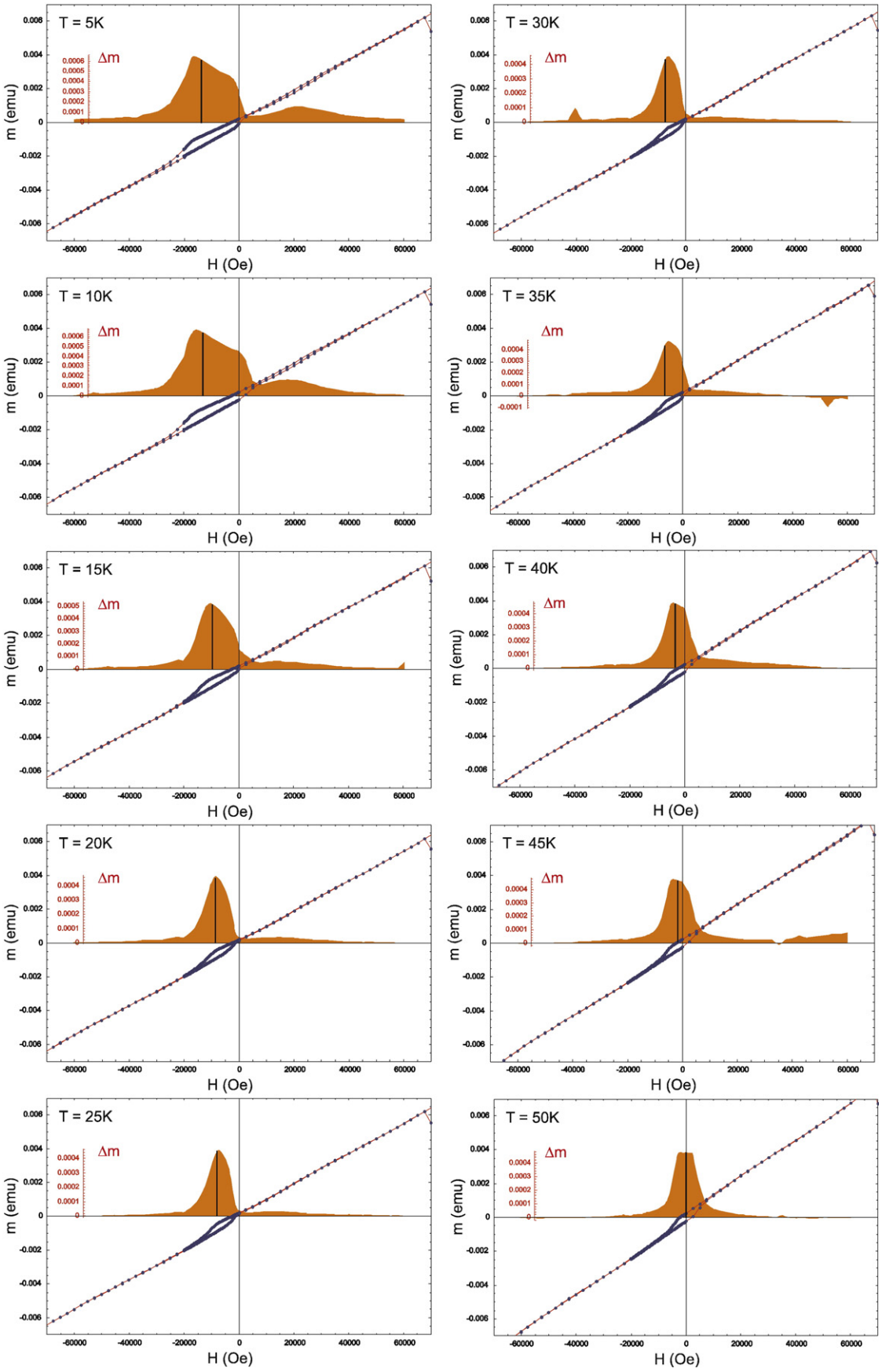

Fig. 6. Hysteresis loops of MODK-4 after cooling a 7 T RT IRM in zero-field to 5 K and stepwise heating to 50 K. Each background displays an amplified plot of the hysteresis difference. The solid line marks the estimated loop shift.

with a He-flow heating inset (Princeton Measurements Inc.). Low-temperature remanences and hysteresis loops in fields up to 7 T were measured at the University of Bremen using a MPMS-XL built by Quantum Design Inc.

2.2. Samples

The measurements were performed on a selection of opaque millimeter-sized oxide grains that were handpicked from a crushed rock sample. The individual grains were optically selected to contain the least impurities. No fields or heavy liquids were applied during the sample preparation, and the maximum spurious or residual instrumental fields the samples have been exposed to are less than 1 mT, well below any noticeable demagnetization field for the Modum rocks (cf. Fig. 4).

2.3. High field LT experiments on IRM

A set of experiments which repeats and extends the measurements of McEnroe et al. (2007b) starts at room temperature. A high field IRM is induced in the samples by applying a field of 7 T for several seconds, and then setting the field back to zero using the no-overshoot option of the MPMS-XL superconducting magnet. The samples are then cooled in zero-field (less than 2 mT) to 5 K. At this temperature a hysteresis loop is measured by reducing an initially applied field of 7 T in equidistant steps of 250 mT down to a threshold field, which has been chosen to be either 2 T, 1 T, or zero-field. Then the field is reduced to a second threshold field (− 1 T or − 2 T) in smaller field steps of 50 mT and to − 7 T in steps of again 250 mT. The same steps are then used during field increase back to 7 T. The resulting hysteresis loops for six different samples are shown in Fig. 5. The amount and distribution of the hysteresis shift is best seen in the hysteresis difference $M_{rh}(H)$, which is obtained by subtracting the lower (ascending) hysteresis branch from the upper (descending) one. This difference contains all information about irreversible magnetization processes during the hysteresis measurements, but cancels all reversible processes, e.g. due to AFM matrix susceptibility or paramagnetic effects.

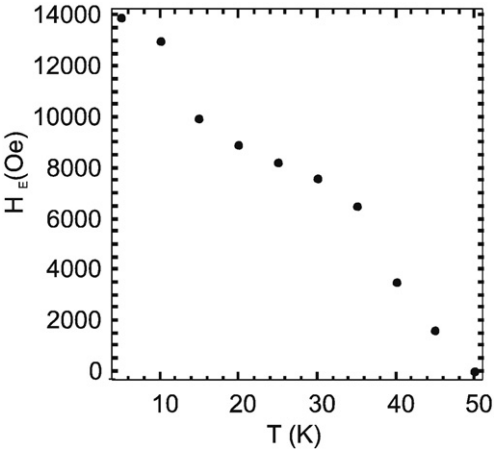

Fig. 7. Temperature dependence of bias field H_E as estimated from the centers of mass of the hysteresis differences in Fig. 6. Exchange bias decreases significantly with increasing temperature and is not detected at 50 K.

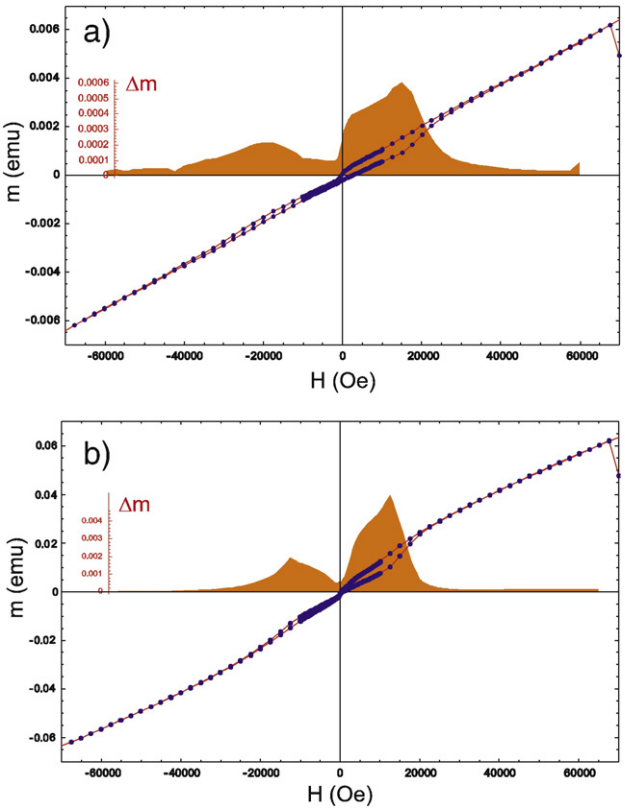

Fig. 8. Hysteresis loops of MODK-4 and MODK-5 after cooling their initial NRM in zero-field to 5 K. The observed loops appear to be superpositions of positively and negatively shifted hysteresis curves. The hysteresis difference is markedly bimodal, where each mode indicates a shift of the same size as observed after IRM cooling. The background displays an amplified plot of the hysteresis difference. In both cases the measured *z*-component of the initial RT NRM was negatively oriented with respect to the instrument co-ordinate system. Accordingly, a positive loop shift is predominant at low temperatures.

The size of the hysteresis shifts and the shape of the hysteresis differences change with the temperature (Fig. 6). The giant shifts at low temperatures have been explained in terms of a strong exchange coupling across uncompensated interfaces between bulk AFM hematite and AFM-ordered ilmenite lamellae.

This has the following rationale:

(1) Shifted hysteresis requires a strong unidirectional anisotropy to be present. This can only be provided by an extremely strongly fixed magnetic moment which favors parallel and disfavors anti-parallel neighboring spins.
(2) A fixing force sufficiently strong to withstand a 7 T field during the hysteresis experiment would need to originate from exchange coupling. Because the loop shift vanishes close to and above the ilmenite-ordering temperature (Fig. 7), AFM ilmenite is an essential agent.
(3) On the other hand, the RT IRM controls direction and intensity of the loop shift. Thus, the original remanence, which at RT is carried by hematite and its contact layers alone, also controls the shift at low temperatures.

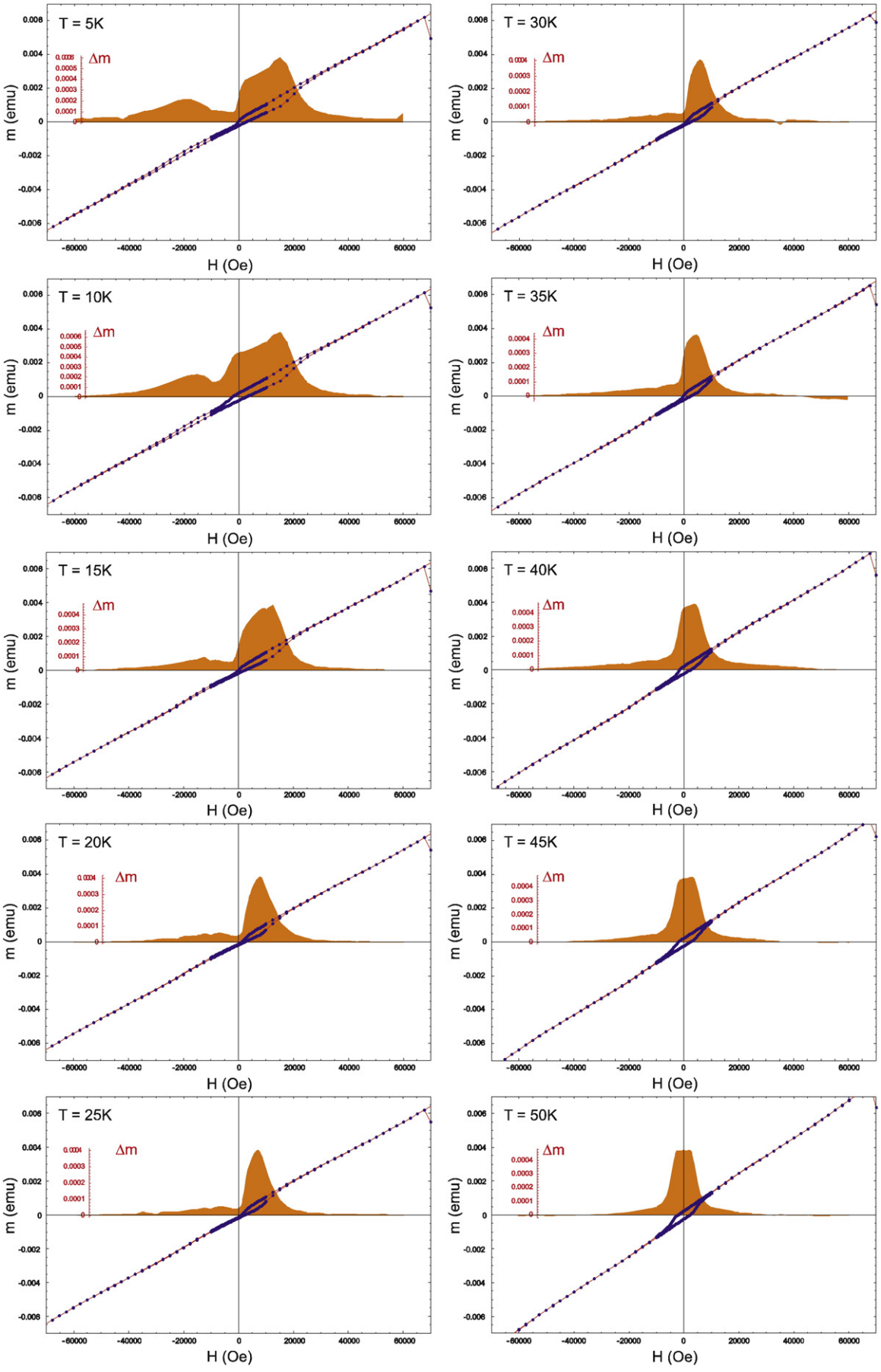
T = 5K
T = 30K
T = 10K
T = 35K
T = 15K
T = 40K
T = 20K
T = 45K
T = 25K
T = 50K
Δm
m (emu)
H (Oe)

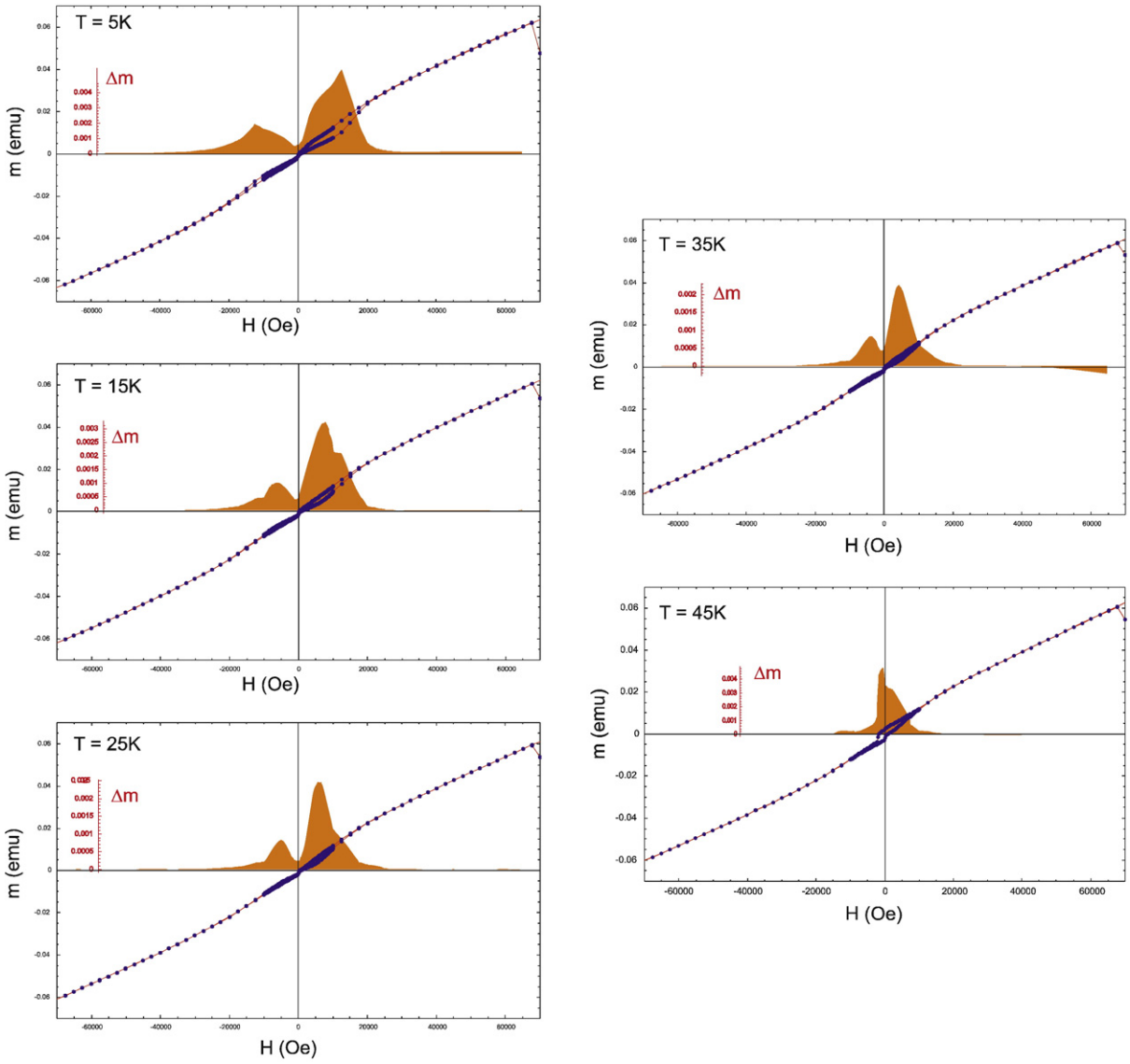

Fig. 10. Hysteresis loops of MODK-5 after cooling their initial NRM in zero-field to 5 K and stepwise heating to 45 K. Each background displays an amplified plot of the hysteresis difference. Exchange bias is significantly decreased with increasing temperature. Both peaks of the bimodal distribution move symmetrically towards the origin with heating.

(4) Shift occurs only in samples showing lamellar exsolution and is apparently more pronounced for fine-scale exsolution. It is therefore most likely related to hematite–ilmenite interfaces.
(5) Because compensated interfaces without net magnetic moment cannot show any field dependence, uncompensated interfaces – or lamellar moments – are the only feasible explanation for the observed loop shifts.

2.4. Zero-field cooling of NRM

Unless a very different explanation for the above IRM experiments can be offered, the existence of lamellar moments in the IRM state can hardly be doubted. Yet, this is not a completely sufficient proof that the original NRM of the sample is also caused by lamellar moments. The classical interpretation would consider the NRM as a TRM or CRM, carried either by the CAF of $FeTiO_3$-substituted hematite, or by defect moments related to lattice defects or local stress centers – as opposed to hematite–ilmenite interfaces.

By extending the previous IRM experiments, by cooling the undisturbed NRM through the ilmenite-ordering temperature down to 5 K, we can decide between the classical interpretation and the lamellar hypothesis of NRM origin. This decision is based on the premise that large hysteresis bias necessarily requires exchange coupling across interfaces. If, as assumed

Fig. 9. Hysteresis loops of MODK-4 after cooling their initial NRM in zero-field to 5 K and stepwise heating to 50 K. Each background displays an amplified plot of the hysteresis difference. Exchange bias is significantly decreased with increasing temperature. Both peaks of the bimodal distribution move symmetrically towards the origin with heating.

by the classical interpretation, the NRM is unrelated to uncompensated hematite–ilmenite interface moments, one then cannot expect to find significant hysteresis bias in a subsequent 5 K hysteresis loop. However, if lamellar moments related to contact layers carry the NRM, a definite bias signal is expected to occur in samples where the RT IRM generates bias. All NRM related measurements, reported in the following, preceded the IRM cooling experiments of the foregoing section.

In view of the above considerations, the overall positive shift of the hysteresis loop in Fig. 8 implies that indeed the NRM participates in the formation of exchange bias, and thus is carried by lamellar surface moments. In fact the positive direction of the shift is inverse to the previously measured negative z-direction of the RT NRM, which is consistent with the fact that a positive RT IRM leads to a negative loop shift.

2.5. NRM-biased loops as a function of temperature

Closer inspection of Fig. 8 indicates that the NRM-induced 5 K loops seem to be the superpositions of smaller, negatively shifted, and larger, positively shifted loops. We interpret this bimodal hysteresis difference as superposition of two structurally similar but quantitatively different lamella populations magnetized in different directions. Each population generates exchange bias, but their biases act in different directions and influence different amounts of magnetization. To support this claim that the NRM is an additive mixture of two inverse populations, the samples were stepwise heated after NRM cooling, and at each temperature a 7 T hysteresis loop was measured. The resulting loops for sample MODK-4 in Fig. 9 show a symmetric movement of the positive and negative peaks of the hysteresis differences. This is consistent with the assumption of qualitatively similar, but quantitatively different populations of inversely exchanged-biased couples. A similar experiment on the NRM of sample MODK-5 in Fig. 10 leads to essentially the same picture.

2.6. Zero-field cooling of partial IRM

Another test of the above two-population hypothesis has been done by producing artificially producing a bimodal hysteresis difference. This was achieved by super-imposing a negative weak field IRM at RT of either − 100 mT, or − 300 mT on a strong positive field IRM acquired in +7 T. This should result in two populations of inversely magnetized remanence carriers with different coercivities at RT. By cooling the resultant remanence subsequently in zero-field to 5 K, each population should generate its own exchange bias. Indeed, after performing these RT partial IRM treatments on sample MODLB-2, the 7 T hysteresis loops at 5 K in Fig. 11 display strong bimodal exchange bias. In both cases the net pIRM at RT was negative, and the two inverse lamellar populations, due to the remanence formation, have very different coercivities at RT, because one population contains the moments which switch below 100 mT (or 300 mT), while the other switches only above this threshold. In spite of this, their induced coercivity distributions of the bias fields are highly symmetric. This hints toward coercivity control by AFM ilmenite at low temperatures.

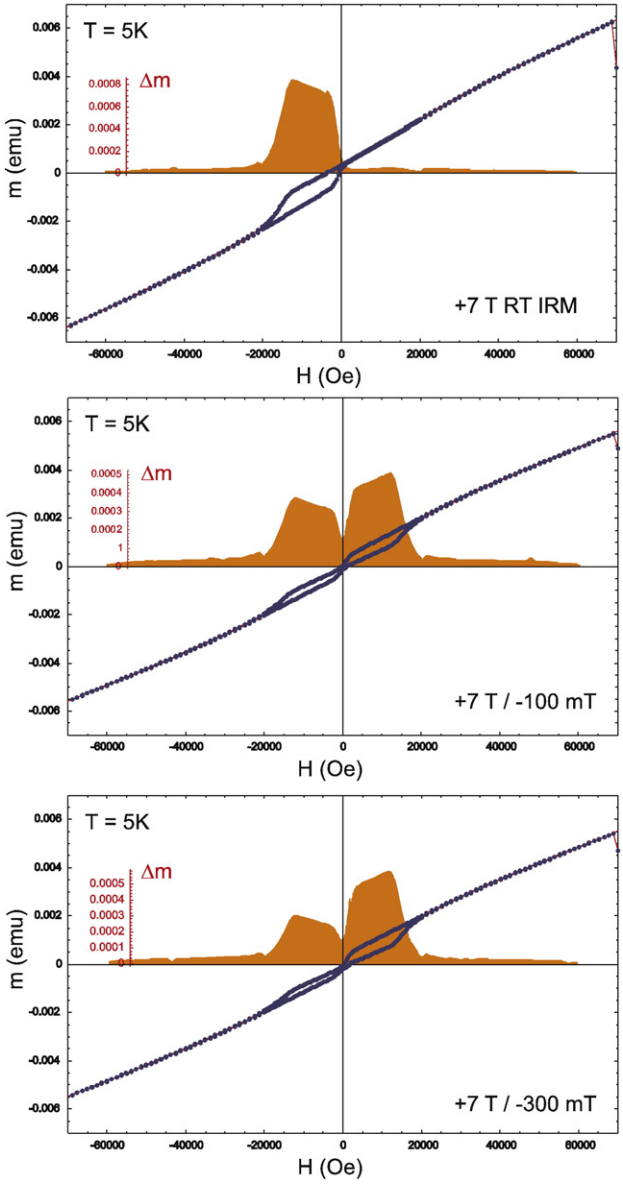

Fig. 11. Hysteresis loops of MODLB-1 and after imprinting a full and partial IRM at RT and zero-field cooling to 5 K. The top panel shows the hysteresis loop of the full IRM at RT after zero-field cooling to 5 K. The second panel shows the hysteresis loop of the first pIRM, obtained by overprinting a +7 T IRM with a − 100 mT IRM at room temperature (top). In the third panel the pIRM was produced using a −300 mT overprint at RT. In these experiments, the negative shift originates from the +7 T IRM magnetization. With addition of a − 100 mT field, the majority of the exchange bias changed to positive, still leaving a significant negative peak. With addition of a −300 mT field, the positive peak is enlarged, and the negative peak is reduced still further.

3. Discussion

3.1. Interpreting remanence-induced exchange bias by exchange coupling across interfaces

The hysteresis shifts observed here are clear evidence of exchange bias by exchange coupling across mineral interfaces.

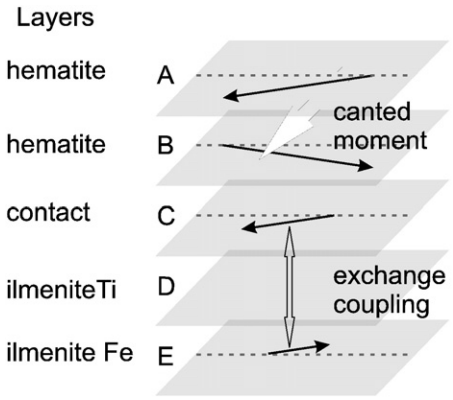

Fig. 12. Sketch of a (0001)-interface region between CAF hematite and ilmenite. Exchange coupling at the interface occurs mainly between Fe-layers C and E. It therefore involves only one of the two anti-parallel hematite spin directions. The CAF moment arises from a <0.07° coherent angular deviation of the hematite spins in layers A and B, and thus is essentially perpendicular within the basal (0001)-plane to both spin directions. Its magnetostatic influence upon the ilmenite Fe-layer is negligible in comparison to the C–E exchange coupling, and cannot explain the occurrence of exchange bias. The arrow in the ilmenite Fe-layer represents only the horizontal component of the magnetic moment. By drawing all moments in plane, this sketch oversimplifies the real situation. In Harrison et al. (2007) a much more detailed model has been proposed, which takes into account that the ilmenite anisotropy favors perpendicular spin orientation leading to an additional torque on all moments.

The fact that a shift occurs only below ilmenite's T_N proves that one of the involved phases is AFM ilmenite. The other phase is the remanence carrier which controls the ordering process of ilmenite when cooling through T_N. This is proven by the direction of shift, which is predominantly opposite to the remanence, whether induced by a RT experiment or by an NRM of untreated grains. The remanence carrier has a T_C close to 610 °C, which fits a titanohematite with about 10% $FeTiO_3$ substitution. Exchange bias is therefore provided by AFM–AFM interfaces between titanohematite and ilmenite. Because both magnetic phases which participate in the exchange bias are AFM, and the bias is opposite to the remanence, this moment must coincide with the titanohematite spin direction directly at the titanohematite–ilmenite interface (see Fig. 12). Therefore, the initial remanence cannot be a spin-canting moment which results from a small equally directed tilt of two opposite spins of adjacent AFM titanohematite layers.

Only one titanohematite layer, the contact layer closest to an ilmenite lamella, provides significant exchange coupling to produce bias. A CAF moment, which is essentially perpendicular within the basal plane to sublattice magnetizations in each single layer, would not lead to a consistent magnetization direction of the adjacent ilmenite Fe-layer. Therefore, a CAF remanence cannot be produced during IRM cooling.

This already is clear evidence that the RT remanence most likely results from unbalanced moments at the interfaces. Because exchange bias definitely requires exchange coupling across a phase boundary, the observations also exclude that the IRM is carried by other minerals, defect moments (not related to ilmenite), or unrelated titanohematites, which, e.g. by magnetostatic coupling, influence the ilmenite ordering.

3.2. Implications for NRM-induced exchange bias

As noted in the last section, the experimental evidence from LT measurements strongly indicates that the natural remanence of the Modum samples is the superposition of two structurally similar but quantitatively different lamella populations magnetized in opposite directions. The envisaged situation is sketched in Fig. 13. These observations are consistent with a feature of the original 'lamellar magnetism' hypothesis of Robinson et al. (2002, 2004), that the remanence is carried by two populations of lamellae which precipitated in-phase and out-of-phase with respect to the local magnetic field. Robinson et al. (2002) assumed that the proportions of these two populations will be highly dependent on crystal orientation of the (0001) basal plane with respect to the magnetizing field at the moment of remanence acquisition during exsolution.

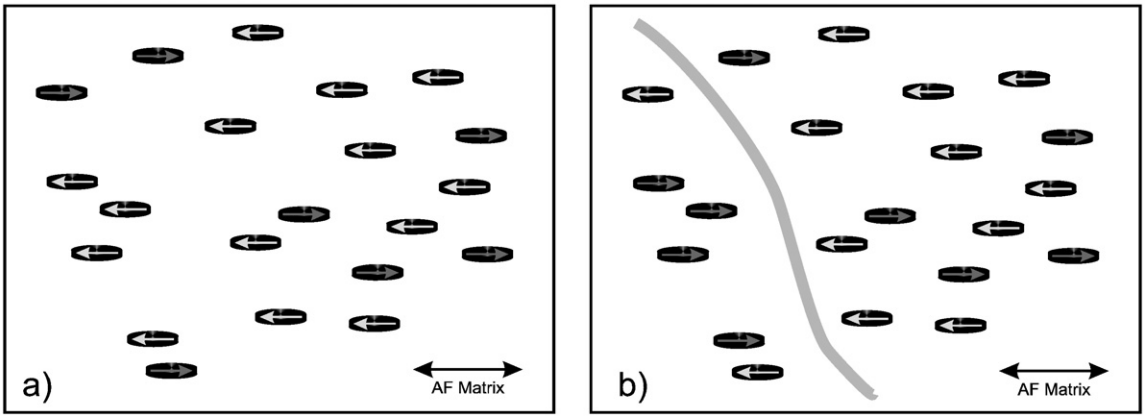

Fig. 13. Conceptional sketch of the two remanence carrying lamella populations. a) The remanence carried by each single lamella arises from uncompensated spins at the interface between hematite host and ilmenite lamella. The spin direction in the AFM host allows only for two different lamellar moment orientations. Which spin direction occurs depends upon the lamella position or the distribution of AFM-domain walls. In b) an 180°-AFM-domain wall (gray line) moved from the left into the sketched region thereby inverting all spins to its left.

The 'two lamellar population'-theory withstands even closest scrutiny. One very remarkable consequence is that the sum of all absolute moments must be the same for NRM and IRM, no matter which equilibrium state the NRM reflects, and no matter which component of the magnetization is measured, e.g. which angle the measurement direction encloses with the axis of lamellar moments. This would be quite different for remanence carriers having more than two different magnetization states.

The above property of lamellar remanence has two quantitative implications which can be directly tested using our LT data: First, because the amount of LT exchange bias generated is independent of the lamellar moment direction, the total hysteresis area must not depend on the ratio between lamellae pointing in positive or negative direction, respectively. Second, the LT coercivity distribution generated by positive and negative hysteresis shifts must be mirror images of each other. This means that the shape of every possible LT loop is the superposition of the LT loop generated by the sample when all lamellae are positively magnetized, and its mirror image. After acquisition of the 7 T RT IRM, the induced bias at 5 K in Fig. 5 closely, but not perfectly, corresponds to complete positive magnetization of all lamellae. By denoting the IRM(NRM)-induced hysteresis difference at temperature T as $M_{\mathrm{rh}}^{\mathrm{IRM}}(T, H)$ ($M_{\mathrm{rh}}^{\mathrm{IRM}}(T, H)$), it is shown in the Appendix that still there is a ratio $0 \le \alpha \le 1$, such that for all temperatures T

$$M_{\mathrm{rh}}^{\mathrm{NRM}}(T,H) = \alpha M_{\mathrm{rh}}^{\mathrm{IRM}}(T,H) + (1-\alpha) M_{\mathrm{rh}}^{\mathrm{IRM}}(T,-H). \quad (1)$$

This relation has been applied to model the NRM-induced hysteresis difference of sample MODK-4 (Fig. 9) in terms of its IRM-induced exchange bias (Fig. 6). By fitting the NRM-induced hysteresis difference $M_{\mathrm{rh}}^{\mathrm{NRM}}$(5 K, H) at 5 K to a sum of the IRM-induced $M_{\mathrm{rh}}^{\mathrm{IRM}}$(5 K, H), and its mirror image $M_{\mathrm{rh}}^{\mathrm{IRM}}$ (5 K, $-H$) according to Eq. (1), the value of $\alpha = 0.12$ has been found. As shown in Fig. 14, it turns out that using this same value of α, a very good fit at all measured temperatures between 5 K and 50 K is obtained. This actually implies that all remanence, NRM- or IRM-induced, at temperatures below 50 K is carried by an ensemble of uniaxial moments which take part in the exchange coupling and produce exchange bias. The recovery experiment in Fig. 3 then shows that about 99% of the RT NRM is of lamellar origin.

3.3. NRM formation by exsolution

The evaluation of our LT measurements leads to the remarkable conclusion that in sample MODK-4 the complete NRM is carried by lamellar moments, and that at least $p = 88\%$ of the NRM

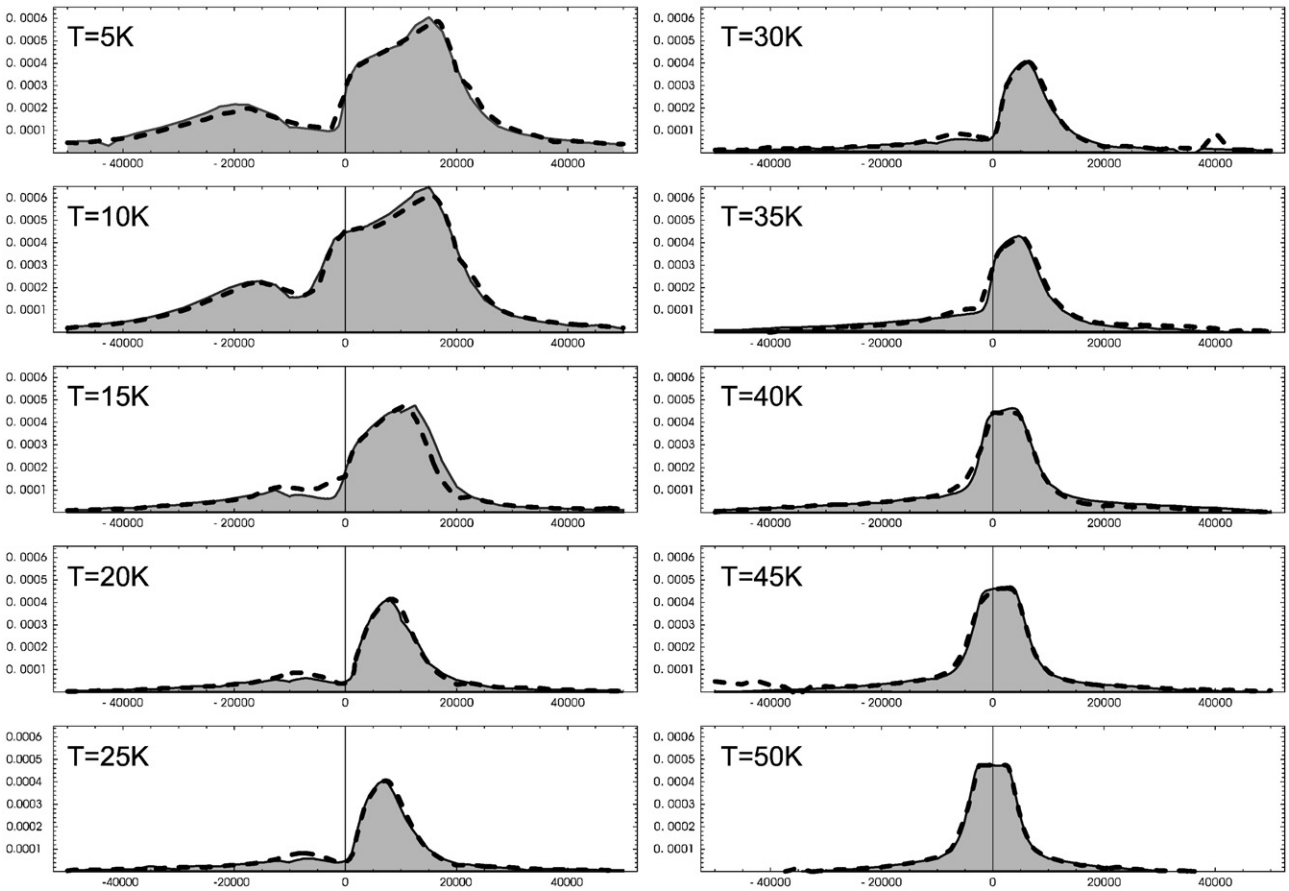

Fig. 14. Comparison between measured (gray shading) and modelled (dashed line) temperature dependence of the NRM-induced hysteresis difference $M_{\mathrm{rh}}^{\mathrm{NRM}}$ (T, H) for sample MODK-4. The model is based on the temperature dependence of the IRM-induced exchange bias $M_{\mathrm{rh}}^{\mathrm{IRM}}$ (T, H), and uses a 12% negatively and 88% positively shifted remanence throughout, resulting from the factor α calculated from the 5 K measurement.

moments which generate exchange bias have a coherent magnetization direction, and only $q=12\%$ are inversely magnetized. In the original NRM, the alignment was probably even better than 88% (up to >95%), because alternating-field demagnetization at RT shows about a 20% remanence increase for typical Modum rocks (see Fig. 4). This indicates the presence of a remanent overprint in the direction of today's normal field. This overprint could be due to low coercivity AFM-domain walls which invert parts of the lamellar population as sketched in Fig. 13b.

In any case, the efficiency of NRM alignment is $p / q \geq 7.3$. The Boltzmann thermodynamic equilibrium predicts an efficiency of

$$p/q = \exp\left(\frac{2\mu H}{kT}\right), \tag{2}$$

where μ is the magnetic moment of an independent unit, and k the Boltzmann constant. In a realistic geomagnetic field strength (50 μT), and at a low blocking temperature of 600 K, this requires either that each independent unit has a moment $\mu \approx 1.8 \cdot 10^7\ \mu_B$, where μ_B denotes the Bohr magneton, or that the thermodynamic equilibrium condition does not apply to the remanence acquisition mechanism.

It is therefore of interest to investigate the possible mechanism of NRM acquisition. The original proposal of lamellar magnetism by Robinson et al. (2004) considered the mechanism sketched in Fig. 15. It starts with a stable solid solution at A. When this solution cools below T_N, it becomes an AFM-ordered phase. If cooling is sufficiently fast, and the nucleation energy barrier $\Delta G_{nucl}(T)$ high, the solid solution undercools metastably to some temperature $T_{exsolve}$ (700 K in Fig. 15 at position B) where $\Delta G_{nucl}(T_{exsolve})$ is low enough to be overcome by thermal energy. At this point (B) diffusion is slow, and mainly nanoscale lamellae form by exsolution to the stable phases C (CAF titanohematite) and D (nearly pure ilmenite).

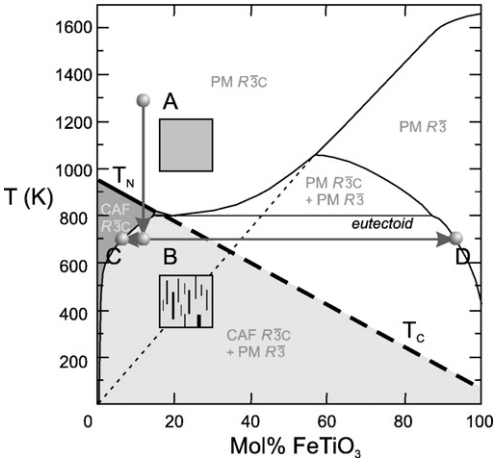

Fig. 15. Simplified sketch of the proposed mechanism of lamellar NRM formation after Robinson et al. (2004). The phase diagram, modified from McEnroe et al. (2007a), delineates crystallographic, as well as magnetic phase boundaries. In the light shaded area a metastable solid solution is magnetically ordered, in the dark shaded area the CAF state is stable. Lamella formation occurs by cooling from A to B. By point B, below the equilibrium curve, nucleation sets in and the metastable solution exsolves into the stable phases at C and D.

Because a magnetic field is present during exsolution, and the titanohematite is magnetically ordered at $T_{exsolve}$, the lamellae prefer positions, where the newly formed lamellar moment is aligned with the effective field-component. During nucleation, the change of a lamellar moment from field alignment to misalignment requires only a one-layer shift of its ilmenite Ti-layers with respect to the titanohematite host (see Robinson et al. (2004), Figs. 8–11).

The kinetics of the lamellar nucleation and aggregation mechanism may systematically favor field alignment and explain the high NRM efficiency, which then needs not follow the naive Boltzmann-statistics above. The simplest model for this is to require that n Ti-atoms have to line up consistently in one layer to fix a new lamella position. For each single Ti-atom the Boltzmann-factor in Eq. (2) then needs to be only $7.3^{1/n}$. This still requires about $n \approx 10^6$ to explain the high total p/q, considering that the uncompensated Fe^{2+}-moment associated with each Ti-atom contributes 4 μ_B to the lamellar moment. However, a more complex lamella growth mechanism by diffusion-limited aggregation could further increase the efficiency of NRM acquisition, although we were not able to find a feasible mechanism which explains a sufficient rise in efficiency with respect to Boltzmann-statistics.

An additional mechanism, which might co-operate with the previous one to yield the high observed NRM efficiency is that remanence, as well as exchange bias, could be produced by exchange-coupled lamellar clusters instead of single isolated lamellae. The physical background of this proposition is that densely clustered lamellae cannot switch independently if the AFM host, which at RT carries the lamellar moment, cannot develop a 180 °-wall between the lamellae. In this case the lamella cluster consists of tightly linked moments which always reverse together and cannot be distinguished from a single isolated moment by macroscopic measurements. If such a cluster typically contains N lamellae and the probability of NRM field-alignment for each lamella is p^*, then the average cluster moment is $\langle m \rangle = N(2p^* - 1)\ \mu$ with standard deviation of $\sigma = 2\mu\sqrt{Np^*(1-p^*)}$. The observed NRM efficiency requires that $\langle m \rangle \approx 2a$, which leads to $N \approx (p^* - 1/2)^{-2}$. When p^* arises from the previous aggregation model of n moments associated with Ti-atoms, an order-of-magnitude estimate for explaining the observed efficiency yields

$$n\sqrt{N} \approx 10^6.$$

While a choice of $n = N = 10000$ fulfills this condition, it still implies a very high efficiency of lamellar aggregation. On the other hand, a smaller aggregation efficiency of $n = 100$ would require already very large clusters ($N = 10^8$). A further problem with the cluster model is, that the average moment of the inverse clusters would be smaller than the moment of the aligned clusters, which should influence the symmetry of the exchange bias experiment. Yet, only very minor symmetry deviations are observed in Fig. 14. These problems provide scope for additional investigation.

In any case, the explanations for lamellar NRM formation considered here indicate that NRM intensity is overwhelmingly

controlled by the details of the mechanisms of lamella formation, which, in turn, depend on cation ordering, Ti diffusion, local chemistry and cooling history. The influence of the external (e.g. geomagnetic) field strength, as opposed to field orientation, upon lamellar NRM appears to be negligible, and highly non-linear. It is an important consequence that lamellar NRM should not be used to obtain even order-of-magnitude estimates for paleofield intensities, whether in terrestrial or extraterrestrial materials.

4. Conclusions

The foregoing investigations lead to the following conclusions:

(1) High-temperature demagnetization indicates that NRM at room temperature is carried by titanohematite-hosted moments, because the NRM is retained to $T_C \approx 610°C$.
(2) Low-temperature demagnetization shows that the Morin transition of hematite is nearly irrelevant, whilst the ilmenite ordering at T_N influences the remanence noticeably. Thus, ilmenite is coupled to the remanence carrying moments.
(3) By cooling the NRM below T_N the sample develops large bimodal exchange bias. Large exchange bias is produced only by exchange coupling across phase boundaries. Therefore, the NRM must be linked to a phase boundary involving ilmenite. Since by Eq. (1) NRM is carried by titanohematite-hosted moments, this must be an interface between ilmenite and titanohematite.
(4) Taken together, the above is just the definition of lamellar magnetism, and proves that the NRM is carried by lamellar moments.
(5) Comparison with partial IRM cooling indicates that the NRM is carried by two competing populations of ilmenite lamellae with opposing moments. The moment ratio of these populations is reflected by the two modes in the hysteresis difference.
(6) The alignment efficiency of 88% versus 12%, estimated thereby, indicates that lamellar NRM acquisition is highly efficient in the measured samples. To model a correspondingly efficient NRM acquisition mechanism, we propose diffusion-limited lamellar aggregation together with exchange-coupled lamellar clusters as independent remanence carriers.
(7) Even though rocks containing lamellar–magnetic minerals may provide a robust record of paleofield orientation, lamellar NRM should not be used for paleointensity estimates, due to the apparent complex and non-linear remanence acquisition.

Acknowledgments

The MPMS measurements for this research were performed with the aid of C. Franke, T. Frederichs, and T. von Dobeneck at the University of Bremen, Germany, and of M. Jackson, P. Solheid, B. Carter-Stieglitz, and S. Banerjee at the Institute of Rock Magnetism, Minneapolis, USA, where they were supported by NSF visitor grants to SM and KF. We wish to thank R. J. Harrison and A. Kosterov for valuable reviews, discussions and comments. We gratefully acknowledge funding through the Norwegian Research Council (NFR, Nanomat), and Petromax, as well as ESF travel grants through the European Mineral Science Initiative (EuroMinScI) of the EUROCORES programme.

Appendix A. Relation between bimodal IRM- and NRM-induced loop shifts

If the LT coercivity distribution of biased loops is generated by positive and negative hysteresis shifts which are mirror images of each other, the shape of every possible LT loop is the superposition of the LT loop generated by the sample when all lamellae are positively magnetized, and its mirror image.

We denote this maximally shifted loop as $M^0_{rh}(T, H)$ and thus have for some ratios $0 \le \beta, \gamma \le 1$:

$$M^{IRM}_{rh}(T,H) = \beta\, M^0_{rh}(T,H) + \overline{\beta}\, M^0_{rh}(T,-H), \tag{3}$$

$$M^{NRM}_{rh}(T,H) = \gamma\, M^0_{rh}(T,H) + \overline{\gamma}\, M^0_{rh}(T,-H), \tag{4}$$

where $\overline{x}$ is defined as $1-x$ for $0 \le x \le 1$. Simple calculation shows then that

$$M^0_{rh}(T,H) = \frac{\beta}{\beta-\overline{\beta}} M^{IRM}_{rh}(T,H) - \frac{\overline{\beta}}{\beta-\overline{\beta}} M^{IRM}_{rh}(T,H). \tag{5}$$

By substituting this in the second line of Eq. (3), one obtains after some simplification Eq. (1) with

$$\alpha = \frac{\beta\gamma - \overline{\beta}\,\overline{\gamma}}{\beta-\overline{\beta}}. \tag{6}$$

References

Balsley, J.R., Buddington, A.F., 1958. Iron titanium oxide minerals, rocks, and aeromagnetic anomalies of the Adirondack area, New York. Econ. Geol. 53, 777–805.

Carmichael, C.M., 1959. Remanent magnetization of the Allard Lake ilmenites. Nature 183, 1239–1241.

Carmichael, C.M., 1961. The magnetic properties of ilmenite–hematite crystals. Royal Soc. London Proc., Ser. A. 263, 508–530.

Hargraves, R., 1959. Magnetic anisotropy and remanent magnetization in hemo-ilmenite from ore deposits of Allard Lake, Quebec. J. Geophys. Res. 64, 1565–1573.

Harrison, R.J., McEnroe, S.A., Carter-Stieglitz, B., Robinson, P., Palin, E.J., Kasama, T., 2007. Low-temperature exchange coupling between Fe_2O_3 and $FeTiO_3$: insight into the mechanism of giant exchange bias in a natural nanoscale intergrowth. Phys. Rev. B 76 (10), 174436.

Hoffman, K.A., 1992. Self-reversal of thermoremanent magnetization in the ilmenite–hematite system — order–disorder, symmetry, and spin alignment. J. Geophys. Res. 97, 10883–10895.

Kasama, T., McEnroe, S., Ozaki, N., Kogure, T., Putnis, A., 2004. Effects of nanoscale exsolution in hematite–ilmenite on the acquisition of stable natural remanent magnetization. Earth Planet. Sci. Lett. 224, 461–475.

Kletetschka, G., Wasilewski, P.J., Taylor, P.T., 2002. The role of hematite–ilmenite solid solution in the production of magnetic anomalies in ground- and satellite-based data. Tectonophys. 347, 167–177.

McEnroe, S.A., Brown, L.L., 2000. A closer look at remanence dominated anomalies: rock-magnetic properties and magnetic mineralogy of the Russell Belt microcline–sillmanite gneisses Northwest Adirondack mountains, New York. J. Geophys. Res. 105, 16437–16456.

McEnroe, S.A., Robinson, P., Langenhorst, F., Frandsen, C., Terry, M., Boffa Ballaran, T., 2007a. Mineral chemistry, phase relations and magnetic properties of hemo-ilmenite ores with micron- to nanometer-scale exsolution lamellae from Allard Lake, Quebec: implications for planetary magnetization. J. Geophys. Res. 112. doi:10.1029/2007JB004973.

McEnroe, S.A., Carter-Stieglitz, B., Harrison, R.J., Robinson, P., Fabian, K., McCammon, C., 2007b. Magnetic exchange bias of more than 1 Tesla in a natural mineral intergrowth. Nature Nanomat. 2, 631–634.

McEnroe, S.A., Harrison, R.J., Robinson, P., Golla, U., Jercinovic, M.J., 2001. The effect of fine-scale microstructures in titanohematite on the acquisition and stability of NRM in granulite facies metamorphic rocks from southwest Sweden: implications for crustal magnetism. J. Geophys. Res. 106, 30523–30546.

McEnroe, S.A., Harrison, R.J., Robinson, P., Langenhorst, F., 2002. Nanoscale haematite–ilmenite lamellae in massive ilmenite rock: an example of 'lamellar magnetism' with implications for planetary magnetic anomalies. Geophys. J. Int. 151, 890–912.

McEnroe, S.A., Harrison, R.J., Langenhorst, F.M.J., Robinson, P., Brown, L., Takeshi, K., 2004a. Exploring effects of nanoscale exsolution on magnetic properties in the hematite–ilmenite series. Geochim. Cosmochim. Act. 68, A101.

McEnroe, S.A., Langenhorst, F., Robinson, P., Bromiley, G.D., Shaw, C.S.J., 2004b. What is magnetic in the lower crust? Earth Planet. Sci. Lett. 226, 175–192.

Merrill, R., 1968. A possible source for the coercivity of ilmenite–hematite minerals. J. Geomag. Geoelectr. 20, 181–185.

Nogués, J., Schuller, I.K., 1999. Exchange bias. J. Magn. Magn. Mater. 192, 203–232.

Nogués, J., Sort, J., Skumryev, V., Surinãch, S., Munõz, J.S., Baró, M.D., 2005. Exchange bias. Phys. Rep. 422, 65–117.

Robinson, P., Harrison, R.J., McEnroe, S.A., Hargraves, R.B., 2002. Lamellar magnetism in the haematite–ilmenite series as an explanation for strong remanent magnetization. Nature 418, 517–520.

Robinson, P., Harrison, R.J., McEnroe, S.A., Hargraves, R.B., 2004. Nature and origin of lamellar magnetism in the hematite–ilmenite series. Am. Mineral. 89, 725–747.

Stamps, R.L., 2000. Mechanisms for exchange bias. J. Phys. D 33, R247–R268.

Wen, G.H., Zheng, R.K., Fung, K.K., Zhang, X.X., 2004. Microstructural and magnetic properties of passivated Co nanoparticle films. J. Magn. Magn. Mater. 270, 407–412.